Geophysical Research Letters

RESEARCH LETTER
10.1029/2021GL092438

Impacts of Engineered Diversions and Natural Avulsions on Delta-Lobe Stability

Brandee N. Carlson[1], Jeffrey A. Nittrouer[1], Travis E. Swanson[2], Andrew J. Moodie[1], Tian Y. Dong[1], Hongbo Ma[1], Gail C. Kineke[3], Minglong Pan[1], and Yuanjiang Wang[4]

[1]Department of Earth, Environmental & Planetary Sciences, Rice University, Houston, TX, USA, [2]Geology and Geography, Georgia Southern University, Statesboro, GA, USA, [3]Earth and Environmental Sciences, Boston College, Chestnut Hill, MA, USA, [4]Yellow River Institute of Hydraulic Research, Zhengzhou, China

Key Points:

- Coastline retreat following channel abandonment is assessed for engineered diversions and natural avulsions on the Huanghe delta (China)
- Antecedent channel topography, riverine water input, and vegetation vary depending on abandonment style, and impact delta lobe stability
- By mimicking conditions for natural channel avulsions, lobes abandoned by engineering practices may be made resilient to shoreline retreat

Supporting Information:

Supporting Information may be found in the online version of this article.

Correspondence to:

B. N. Carlson,
brandee.n.carlson@vanderbilt.edu

Citation:

Carlson, B. N., Nittrouer, J. A., Swanson, T. E., Moodie, A. J., Dong, T. Y., Ma, H., et al. (2021). Impacts of engineered diversions and natural avulsions on delta-lobe stability. *Geophysical Research Letters*, *48*, e2021GL092438. https://doi.org/10.1029/2021GL092438

Received 7 JAN 2021
Accepted 31 MAY 2021

Abstract Reduced sediment supply and rising sea levels are driving land submergence on deltas worldwide, motivating engineering practices that divert water and sediment to sustain coastal landforms. However, lobe response following channel abandonment by diversions has not been constrained by field-scale studies. Herein, avulsion and engineered diversion scenarios are explored for the Huanghe delta (China), where three lobes were abandoned in the last 40 yr. Two lobes were completely cut off by diversions, and one naturally by an avulsion. Shoreline retreat rates are strikingly different: ~400 m/yr for diverted lobes and ~90 m/yr for avulsed lobe. We hypothesize that this variability is linked to vegetal cover across lobes, and therefore the capacity to buffer hydrodynamic reworking of shoreface sediment. Furthermore, the vegetal cover is related to lobe salinity and elevation, which vary by abandonment style. We offer this as a case study to inform about the efficacy of future delta diversions.

Plain Language Summary Sediment and water diversions are an important tool to combat land loss of deltaic coastlines. However, nourishment of drowned coastal land typically requires diverting water and sediment away from another region of the coast, potentially resulting in additional land loss. This study finds that the stability of shorelines facing reduced sediment supply is dependent on elevation before sediment loss, freshwater supply, and vegetation coverage. These findings have implications for future sediment and water diversions, by informing strategies that optimize land preservation.

1. Introduction

The dispersal of sediment to deltaic coastlines is partially controlled by avulsion processes, whereby an active channel is abandoned rapidly in favor of a new course. Consequently, avulsions redistribute water and sediment to construct a new lobe (Kim, 2012; Kim et al., 2009; Paola et al., 2011). Avulsions typically arise due to sediment aggradation on the channel bed relative to adjacent channel levees and are often triggered by river floods (Mackey & Bridge, 1995; Mohrig et al., 2000). In deltaic systems, avulsions usually occur at the hydrodynamic transition to backwater flow and happen on timescales of decades to millennia (Ganti et al., 2014; Nittrouer et al., 2012). An avulsion may result in a new channel pathway carved on the delta floodplain, or the re-occupation of a previously abandoned distributary channel (Slingerland & Smith, 2004). In either case, channel relocation results in sediment delivery to a different part of the coastline, where land building may begin in earnest. Meanwhile, the abandoned lobe typically experiences shoreline retreat due to reduced sediment supply in the face of wave and tidal reworking of sediment (Roberts, 1997).

At present, many deltaic coastlines are experiencing land loss due to accelerating rates of sea-level rise, enhanced subsidence due to fluid extraction, and reduced sediment supply (Blum & Roberts, 2009; Giosan et al., 2014; Hoitink et al., 2020; Syvitski et al., 2009). Because deltas host a large proportion of human population and are economically valuable, channel diversions have been implemented, or are considered, as a viable engineering tool to combat coastal land loss. The goal is to relocate water and sediment dispersal to areas that require maintenance of the subaerial landform (Paola et al., 2011). As such, recent attention has been paid to understanding the growth of developing delta lobes. A prime example of such activity includes the Wax Lake Delta of Louisiana, USA, which was initiated by a diversion from the Atchafalaya

River in 1941. A delta emerged subaerially in the Atchafalaya Bay by 1973, exemplifying land building through a co-organization of delta substrate, channels, levees, and vegetation (Shaw & Mohrig, 2014; Wagner et al., 2017).

Delta morphology responds dynamically to river floods (Hiatt et al., 2019; Olliver et al., 2020), ocean storms (Xing et al., 2017), tides (Hoitink et al., 2017; Shaw & Mohrig, 2014), subsidence (Syvitski et al., 2009; Törnqvist et al., 2008; Wilson & Allison, 2008), waves (Gao et al., 2020; Nienhuis et al., 2013), and vegetation, through coupled eco-geomorphic feedbacks that impact sediment deposition and erosion (Gosselink et al., 1998; Olliver et al., 2020; Paola et al., 2011; Piliouras et al., 2017). For example, numerical modeling studies have assessed shoreline response to fluvial abandonment, and demonstrated that wave-driven alongshore sediment transport reworks abandoned lobe sediment, smoothing the shoreline (e.g., Nienhuis et al., 2013). However, few field-based observational studies have investigated shoreline response to factors including a rapid reduction in sediment supply, variable surface topography, vegetation, and riverine freshwater supply.

Herein, this study investigates the Huanghe (Yellow River) delta, a system with multiple lobes recently abandoned by both engineering practices and natural avulsions, to evaluate mechanisms that influence shoreline stability of abandoned deltaic lobes. Detailed field and remote sensing observations are combined to assess the roles of waves, topography, riverine water input, and vegetation, correlating these factors to lobe retreat rates after a restriction of water and sediment supply.

1.1. Variable Lobe Characteristics and Retreat Rates of the Huanghe Delta

The Huanghe extends from the Tibetan Plateau, across the North China Plain, and terminates at the Bohai Sea (Yu, 2002). Along its path, the Huanghe is enriched in sediment as it crosses the Loess Plateau, which is comprised of easily erodible silt and very fine sand (Yu, 2002). The high sediment load of the Huanghe generates rapid dynamics in its lowermost reaches, and the Huanghe changes its course via channel abandonment approximately every decade (Figure 1b). As a consequence, the delta system is constructed of multiple lobes, whereby one develops at the mouth of the active channel. Once abandoned, the lobe is subjected to sediment reworking by waves and tides, resulting in shoreline retreat.

In the past 70 yr, multiple engineered diversions have been implemented on the Huanghe delta, typically in anticipation of an impending natural avulsion. For example, in 1976, the Diaokou Channel was abandoned, and in 1996, the Qingshuigou Channel was abruptly rerouted (Figure 1b). In both cases, riverine connection to the abandoned lobes was severed, allowing no upstream water or sediment to reach the abandoned channels. As a result, the channels were left as low-elevation scars, and the lobes subject to reworking (Carlson et al., 2020). As recent studies have explored, sediment of the eroding lobe fills the abandoned channel. Over time the antecedent topography of the channel is reworked and converted into a mudflat (Carlson et al., 2020; Li et al., 2020; Wu et al., 2020). In the studied delta lobe, this is facilitated by a tidal channel network that extends from the shoreline into the abandoned channel, conveying sediment-laden water landward during rising tides. Material subsequently deposits during slack-tide conditions, filling the antecedent channel topography with mud (Carlson et al., 2020). Presently, the Qingshuigou mudflat possesses limited vegetation coverage across its mudflats, with exception of sporadic colonies of saline-tolerant *Suaeda salsa* (*S. salsa*). Atop the adjacent antecedent channel levees, and above tidal inundation, *Phragmites Australis* (*P. australis*) is abundant.

Natural avulsions on the Huanghe delta take several years to complete. Typically, an avulsion is characterized first by crevassing events, followed by the sustained levee-breaching flow that manifests into a new channel, thus completing the process (Hajek & Edmonds, 2014; Jones & Hajek, 2007). For example, over a multiple-year period (2005–2007), an avulsion relocated the Qingba channel ~5 km northward (Figure 1b). Following the avulsion, a tie channel continued to convey water and sediment from the active channel to the abandoned Qingba lobe. This tie channel extends across the antecedent channel and connects to a tidal channel approximately halfway between the avulsion node and the modern shoreline (Figure 1e). Presently, *P. australis* occupy ~2 km adjacent to the avulsion node, along the abandoned channel path. Nearing the shoreline, vegetation becomes increasingly saline-tolerant, and species such as *S. salsa* and *S. alterniflora* are abundant.

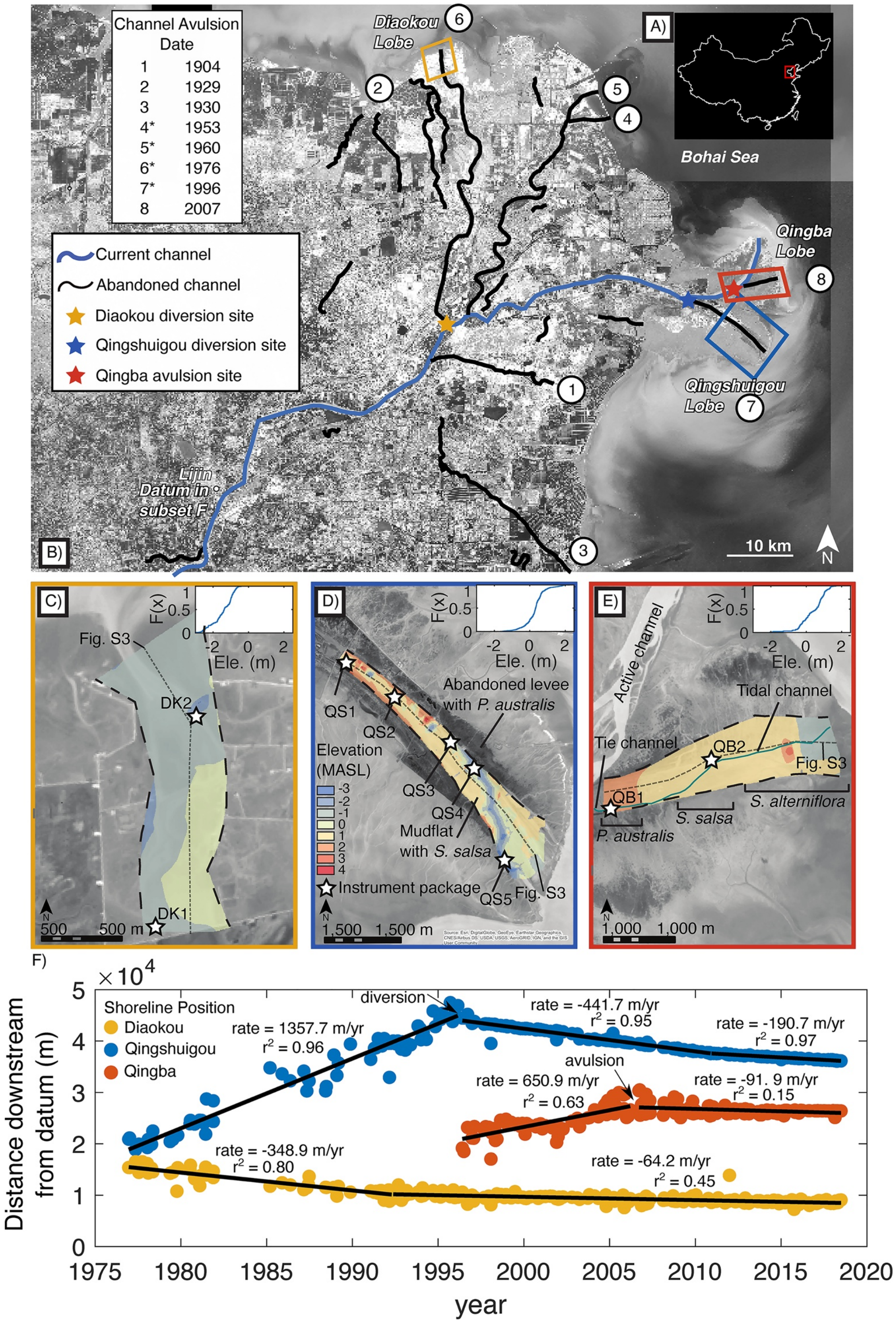
Channel Avulsion Date
1 1904
2 1929
3 1930
4* 1953
5* 1960
6* 1976
7* 1996
8 2007
Current channel
Abandoned channel
Diaokou diversion site
Qingshuigou diversion site
Qingba avulsion site
Diaokou Lobe
Bohai Sea
Qingba Lobe
Qingshuigou Lobe
Lijin Datum in subset F
10 km
A)
B)
C)
D)
E)
F)
Fig. S3
DK2
DK1
500 500 m
F(x)
Ele. (m)
QS1
QS2
QS3
QS4
QS5
Abandoned levee with P. australis
Elevation (MASL)
Mudflat with S. salsa
Instrument package
1,500 1,500 m
Active channel
Tidal channel
Tie channel
QB1
QB2
S. salsa
S. alterniflora
P. australis
1,000 1,000 m
Shoreline Position
Diaokou
Qingshuigou
Qingba
diversion
avulsion
rate = 1357.7 m/yr
r² = 0.96
rate = -441.7 m/yr
r² = 0.95
rate = -190.7 m/yr
r² = 0.97
rate = 650.9 m/yr
r² = 0.63
rate = -91. 9 m/yr
r² = 0.15
rate = -348.9 m/yr
r² = 0.80
rate = -64.2 m/yr
r² = 0.45
Distance downstream from datum (m)
×10⁴
year

Figure 1

The shoreline positions of the Diaokou, Qingshuigou, and Qingba lobes were tracked using 299 satellite images obtained from Landsat between the years 1976–2018, and by assessing the movement of the channel centerline following abandonment using the methods of Moodie et al. (2019). The Diaokou and Qingshuigou lobes demonstrate consistent retreat rates for about one decade following abandonment: 349 m/yr and 442 m/yr, respectively (Figure 1f). Interestingly, a decade after abandonment, retreat rates for both lobes relaxed: by 1990, the Diaokou lobe was 64 m/yr, and by 2007, the Qingshuigou was 190 m/yr. In stark contrast is the magnitude and style of retreat for the Qingba lobe (natural avulsion): it has maintained a consistent retreat rate of 92 m/yr since abandonment in 2007 (Figure 1f).

1.2. Exploring Influences of Waves, Topography, Riverine Water, and Vegetation on Lobe Retreat

The discrepancies in shoreline retreat rates for Huanghe delta lobes may be contextualized by abandonment style: engineered diversion vs. avulsion. In particular, we ask the following questions: Could retreat rates be traced to differences in lobe properties? And, are lobe properties connected to abandonment style? This is explored by assessing potential differences in wave climate, antecedent topography, riverine water input, and vegetation for each of the three lobes. As informed by previous studies, we hypothesize that these are primary controls affecting shoreline stability, however, they are not independent of one another. For example, elevation of deltaic deposits impacts hydroperiod (duration and frequency of wetting), as well as salinity, by affecting tidal inundation, both of which influence vegetation species (Gosselink et al., 1998). In turn, vegetal cover imparts eco-geomorphic feedbacks that mediate hydrodynamic energy and sediment transport (Luhar & Nepf, 2013; Nepf, 1999; Nepf & Vivoni, 2000; Piliouras et al., 2017). Here, we examine these and other considerations for each of the three lobes.

1.3. Wave-Driven Reworking of Delta Lobes

Alongshore sediment transport was simulated for the Huanghe delta to assess shoreline response of deltaic lobes forced by two wave classes: 1) fair weather, and 2) storm waves. Simulations were carried out using a Shoreline Simulation model (ShorelineS), a free-form (i.e., vector-based) model that predicts shoreline displacement driven by variable wave information (Roelvink et al., 2020). Information about how ShorelineS computes shoreline motion is found in Supporting Information (Text S4). Critical input parameters were determined based on field studies, and time-continuous measurements (Text S3–S5); specifically, fair-weather waves and significant wave height ($Hs_0 = 1$ m), wave period ($T = 5$ s), and the deep-water wave angle ($\phi_0 = 175°$, i.e., waves propagate from the south). The storm wave class is defined using $Hs_0 = 4$ m, $T = 8$ s, and $\phi_0 = 64°$ (approximately northeast). A detailed table of modeling parameters is available in Supporting Information (Table S1). Simulations were run for each lobe over one-day period, considering the shoreline position of the Diaokou, Qingshuigou, and Qingba lobes, so that wave climate and coastal orientation drive wave approach angle. It should be noted that the results are not calibrated, as field measurements of alongshore transport are not available. Generally, short-term changes in shoreline position are thought to be driven by changes in shoreface slope. We test the hypothesis that lobe shape and alignment with storm vs. fair-weather waves could be responsible for the contrast in lobe responses to avulsion and diversions (Figure 2).

The simulated shoreline responses demonstrate interesting contrasts between lobe shoreline displacement as affected by fair weather and storm waves (Figure 2). All simulations generate a response that varies along

Figure 1. (a) Outline of China with the location of the Huanghe delta outlined by the red box; (b) a Sentinel-2 satellite composite of the Huanghe delta, assembled from images spanning November, 2017–June, 2020. The modern course (blue) mapped with previous courses (black), and the location of the three deltaic lobes highlighted with colored boxes; the location of the respective avulsion nodes is also indicated by the colored stars; (c) the Diaokou, (d) Qingshuigou, and (e) Qingba abandoned lobes, indicating elevation with respect to mean sea level. Elevation data are also displayed as a cumulative distribution function in the top right corner of (c–e). Dashed gray lines denote the location of channel-centerline elevation transects depicted in Figure S3. White stars indicate the locations of deployed instrument packages; (f) measured shoreline position (with reference to an upstream datum) and time, for the three abandoned lobes studied herein. *Note*. data color coincides with box colors above. Piecewise linear regression functions to the data indicate the rates of changes measured for each shoreline position. The Qingshuigou diversion in 1996, and the Qingba avulsion in 2007 are set as breakpoints for the regressions. The breakpoints for the relaxation in retreat rates for Diaokou and Qingshuigou following diversions are determined by minimizing the residual sum of squares for each fit.

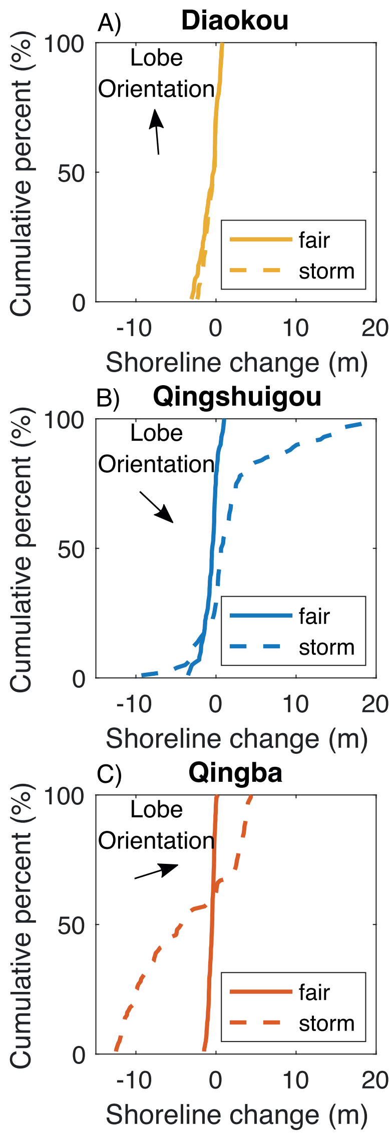

Figure 2. The daily output of shoreline change simulated for fair and storm wave conditions for the three studied Huanghe delta lobes. (a) The Diaokou lobe exhibits shoreline retreat for both conditions; (b) the Qingshuigou lobe moves little under the influence of fair-weather conditions, while storm conditions produce regions of shoreline progradation and retreat. (c) The Qingba lobe shows slight retreat for fair conditions; however, storm conditions generate a large retreat. The Diaokou (north facing) lobe is predicted to retreat the least, while the Qingba is expected to change the most. Both predictions run contrary to observations (Figure 1F).

the shoreline, and results are plotted as cumulative distribution functions to highlight the range of predicted shoreline behavior. During fair-weather conditions, Diaokou is predicted to exhibit retreat (Figure 2a). Interestingly, storm-wave conditions result in less landward retreat than fair-weather wave conditions. Conversely, along the Qingshuigou lobe, fair-weather waves generate a tightly distributed near-zero daily change in shoreline position. Storm waves drive seaward progradation of the Qingshuigou lobe, though some regions of the shoreline exhibit retreat (Figure 2b). During simulated fair-weather waves, the Qingba lobe exhibits small and tightly distributed rates of landward retreat (Figure 2c). Storm waves vastly augment shoreline retreat rates (>10 m/day) and drive portions of the lobe to prograde seaward (Figure 2c). Observations of shoreline retreat through time indicate relatively high shoreline retreat for both the Diaokou and Qingshuigou lobes compared to the Qingba lobe, which is inconsistent with modeling results (Figure 1f). The model prediction that the Qingba lobe is sensitive to changes from fair-weather to storm wave conditions is counter to observation and suggests that, with all parameters constant other than shoreline orientation and wave approach angle, there could be unaccounted factors that accelerate erosion of lobes abandoned by diversion, or buffer erosion of the Qingba lobe.

1.4. Antecedent Topography of the Abandoned Channel

Subtle topography gradients are important for influencing salinity and hydroperiod on deltas (Johnson et al., 1985; Paola et al., 2011). The maximum delta topset relief is generally small and is assessed as the difference in height between the channel thalweg depth and the adjacent levee crest. For the Huanghe system, this is ~3 m. Based on the measured (modern) elevation of the three lobes, we find differences between those abandoned by diversion vs. avulsion. Specifically, the mean elevation of the Qingba lobe is higher compared to the Diaokou and Qingshuigou lobes (Figures 1c–1e). This is evident in the fact that the latter two are largely intertidal, while a large portion of the Qingba lobe remains supratidal.

To assess the role that fluvial processes play in establishing patterns of topography, the Qingshuigou and Qingba channels and lobes prior to abandonment were assessed using the modified normalized difference water index scheme (Xu, 2006). Wetted vs. dry surfaces were determined based on satellite images just before channel abandonment, with a comparison between the two channels conducted for similar riverine water discharges. Both channels possessed similar widths (~1,000 m), consistent with the modern active channel. As measured levee-to-levee, the proportion of subaerial channels present in the Qingshuigou and Qingba channels, respectively, was 15% and 30% (Text S6, Figure S9). Based on expression, these subaerial deposits are presumed to be fluvial bars. In the Qingba channel, these bars were concentrated just downstream of the avulsion node prior to abandonment. Today, the location of the antecedent bars corresponds to the region of topographic highs in the abandoned channel (Figures 1e and S9).

1.5. Riverine Versus Tidal Inundation of the Abandoned Lobes

For deltas, hydroperiod dictates vegetal cover and therefore eco-geomorphic feedbacks (Gosselink et al., 1998). We therefore monitored variation in water depth, flow velocity, and salinity of the modern tidal and tie channels of the abandoned lobes using pressure transducers (PTs), tilt current meters (TCMs), and conductivity loggers (CLs; Text S5 for full field methods). In the Qingshuigou tidal channel, five sets of PTs and TCMs were co-located for 19 days, with three of these instrument suites having a CL. Two PTs were deployed in the Diaokou tidal channel for 12 days. In Qingba, two instrument suites consisting of a PT, TCM, and CL were deployed for 15 days: one in the tie channel, proximate to the active channel junction, and another at the transition downstream to the tidally influenced channel, located approximately halfway between the avulsion node and modern shoreline (Figures 1c–1e).

Water depth variations due to tides were identified at all locations: tides were mixed and semi-diurnal. Tidal ranges (spring tide) recorded at Diaokou and Qingshuigou were 2.3 and 1.6 m, respectively. Bi-directional flow prevailed throughout the Qingshuigou tidal channel, with maximum flood velocity measuring 0.7 m/s, and maximum ebb velocity measuring 0.9 m/s. Salinity ranged 7–37 PSU. For the Qingba lobe tie channel, flow was unidirectional (downstream), the tidal range was 0.5 m, maximum velocity was 0.1 m/s, and salinity did not measure above 1 PSU. At the tie-tidal channel transition, flow was bi-directional, the tidal range was 1.1 m, and salinity ranged 4–18 PSU (Text S5, Figure S8).

1.6. Vegetation Coverage of the Abandoned Lobes

Vegetation impacts hydrodynamics and sediment transport, and so vegetal cover for the three lobes were evaluated using a Normalized Difference Vegetation Index (NDVI) (Kerr & Ostrovsky, 2003; Shao et al., 2016; Sun et al., 2018), sampled bi-monthly, from 410 cloud-free Landsat images collected 2000–2019, over an area ranging 5–7 km^2 near the shoreline. The area close to the shorelines of the Diaokou, Qingshuigou, and Qingba lobes shows stark differences (Figure 3). For the Diaokou lobe, NDVI for all months are near zero, indicating no vegetation, only bare ground. The NDVI values for the Qingshuigou lobe shoreline progressively decrease over time, indicating that since 2000, the lobe has been losing vegetation. In contrast, the NDVI values for the Qingba lobe increase over time; in particular, the lobe gains vegetation after abandonment in 2007 (Figure 3).

2. Discussion

Channel avulsions redistribute sediment to delta coastlines, and therefore offer insights into best practices for designing and implementing large-scale water and sediment diversions that can be used as a tool to promote coastal resiliency. Sediment diversions may be designed to completely cut off water and sediment to a previously active channel, such as those engineered on the Huanghe delta (i.e., the Diaokou and Qingshuigou diversions), or to provide continued connection to the primary channel, such as those outlined in the *Louisiana's Comprehensive Master Plan for a Sustainable Coast* (Coastal Protection & Restoration Authority, 2017). In either case, diversions offer a mixture of human engineering and nature-based solution to enhance natural delta-building processes. The duality of the Huanghe diversions and avulsion can be used to inform techniques that optimize sediment retention and landform stability.

Over several decades, the Huanghe has been subject to diversions that completely sever water and sediment to previously active channels, as well as avulsions, which maintain a persistent (albeit limited) connection between the primary and abandoned channels. The shorelines of the two lobes abandoned by diversions (Diaokou and Qingshuigou) retreated at rates four times faster than the lobe abandoned by avulsion (Qingba). Attributes of each lobe, including reworking during fair/storm wave conditions, measurements of topography, access to fresh (riverine) water, and vegetal cover, all contrast. Interestingly, the orientation of the Huanghe delta lobes relative to wave conditions does not account for differences in shoreline retreat rates. We therefore focus on the other important attributes absent from the modeling framework to understand why ShorelineS model results fail to predict observations. We assess the above-described attributes and discuss how avulsed channel lobes are resilient to shoreline retreat compared to lobes deserted by engineering practices.

2.1. Abandonment Style: Elevation and Water Input

Mean elevation of the Diaokou and Qingshuigou antecedent channels is lower than Qingba. Diaokou and Qingshuigou were abandoned in 1976 and 1996, respectively. In part, elevation change is a product

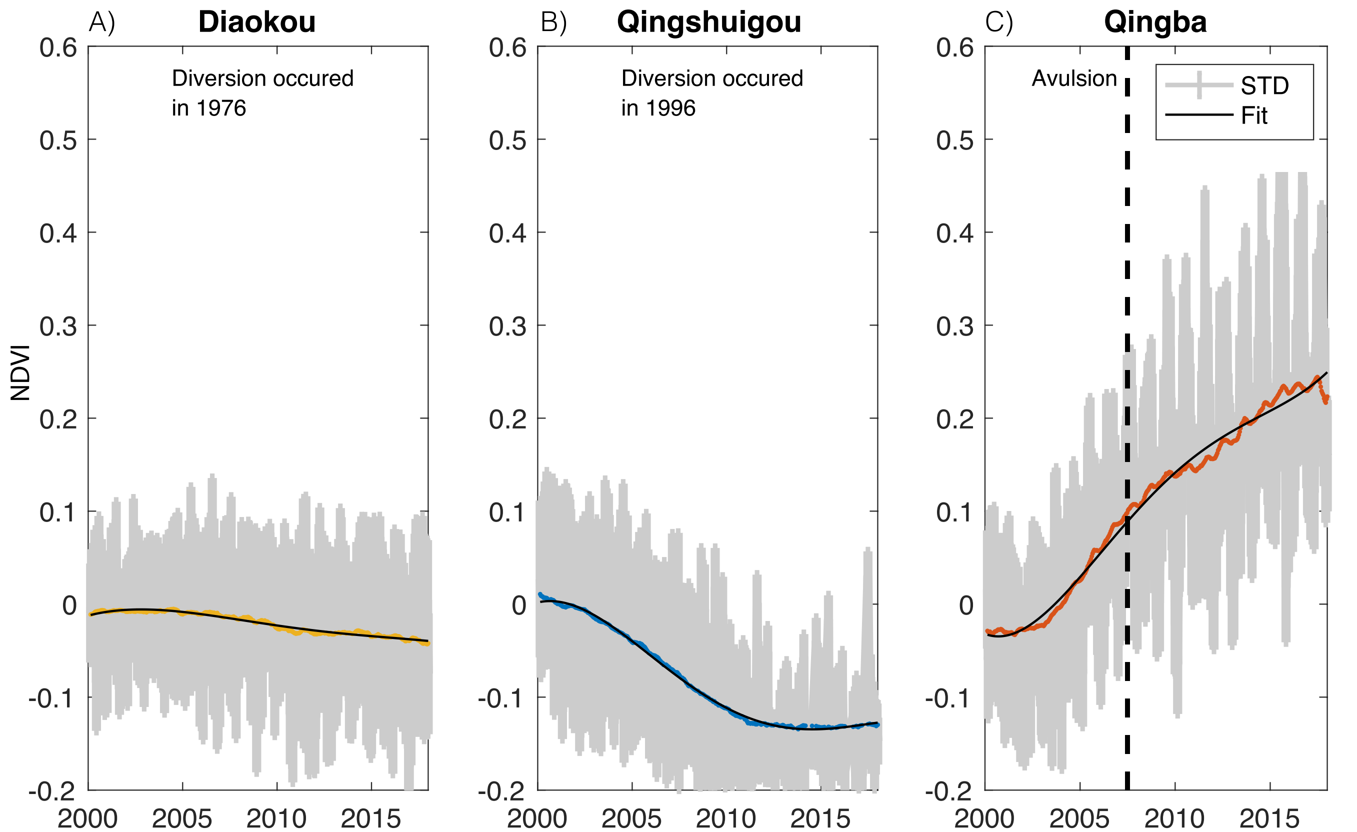

Figure 3. The Normalized Difference Vegetation Index (NDVI) plotted over time (2000–2019) for the; (a) Diaokou, (b) Qingshuigou, and (c) Qingba lobe shorelines, outlined in Figure 1b. NDVI data are smoothed using a moving average with a 12-months window, and the resulting average is plotted as the solid-colored line. The standard deviation of the averaged NDVI values is shown by the gray envelope, and the NDVI values are fit with a polynomial function, displayed as the solid black line. NDVI values for the Diaokou shoreline are consistent and show values less than 0.2, indicating that the abandoned channel is consists of bare (muddy) ground. (b) The NDVI values for the Qingshuigou lobe decrease over time. (c) NDVI values for the Qingba lobe are relatively low prior to avulsion (2007, as indicated) but increase over time: what was once a continuously wetted channel bed transitions to significant vegetation. Negative NDVI values indicate barren areas, including ground covered by rock, sand, snow, or water.

of multiple decades of subsidence. Deltas are low-sloping landscapes with little topographic relief and as such subsidence can have profound impacts on shoreline retreat rates (Törnqvist et al., 2008; Wilson & Allison, 2008; Zhang et al., 2014). The impact of subsidence on Huanghe delta lobe shoreline retreat can be gauged by using a maximum annual subsidence rate (25 mm/yr; Zhang et al., 2014) to compute land surface lowering since the time of abandonment. For example, the Diaokou, Qingshuigou, and Qingba lobes could have lowered by as much as 100, 50, and 25 cm, respectively. Hence, the maximum elevation discrepancy due to subsidence between abandoned lobes is estimated to be 75 cm. The maximum difference in median elevations among the three delta lobes is 193 cm (i.e., calculated using median elevations of −137, 33, and 56 cm above sea level for Diaokou, Qingshuigou, Qingba lobes, respectively). As such, subsidence could account for ~40% of the observed elevation difference (i.e., 75 vs. 193 cm) and therefore the mean elevation differences between the three channels are larger than the difference in elevation due to subsidence. Measured elevation variability between lobes is linked instead to antecedent channel bed topography, with possible feedbacks to vegetation and sediment deposition.

Satellite imagery indicates fluvial bars were concentrated in the Qingba channel before abandonment, particularly near the avulsion node (Figure S9). As measured directly, this area maintains high topography (Figure 1e). We assert that the Qingba channel underwent a natural channel avulsion as a consequence of sediment aggradation on the channel bed, which from 2005 to 2007 initiated crevassing and, ultimately, desertion of the Qingba channel in favor of the modern distributary channel. In contrast, engineered

10.1029/2021GL092438

diversions are an instantaneous cutoff at a prescribed location, and abandoned channels possess a relatively low elevation profile.

Abandonment style and subsequent elevation of the channel influence the nature of freshwater and sediment input (Gaweesh & Meselhe, 2016). Large portions of the Qingba lobe remain supratidal and as such are not regularly inundated by saline (marine) water. Moreover, a tie channel conveys freshwater to this lobe. In contrast, the low relief Diaokou and Qingshuigou channels are intertidal and inundated diurnally by saline water and remain devoid of freshwater input without connectivity to the active channel. Deltaic distributary channels abandoned by avulsion often retain a tie channel that connects to the primary channel. This is consistent with observations of deltas that evolve over longer timescales than the Huanghe: the Mississippi River delta system experiences major lobe abandonment over centuries to millennia, and its bayou network is an example of a persistent connection between the main and abandoned channels (e.g., bayous LaFourche, Maringuoin, and Teche; Roberts, 1997). Similar examples exist for other river delta systems covering a range of sizes (e.g., Brazos River delta, Taha & Anderson, 2007; Selenga River delta, Dong et al., 2020). Even in lowland river systems, tie channels maintain a persistent freshwater connection to abandoned channels (Day et al., 2008; Rowland et al., 2009, 2005).

2.2. Vegetation, Shoreline Stability, and Informing Engineering Strategies

As deltaic land builds over time, plant coverage typically increases (Gosselink et al., 1998; Johnson et al., 1985). In the case of the Qingba lobe, total plant cover has continued to increase despite a shoreline retreat rate of 92 m/yr since abandonment (Figure 3). NDVI data indicate that soon after avulsion, *P. australis*, *S. alterniflora*, and *S. salsa* established rapidly within the abandoned channel. Antecedent fluvial bars (local topographic highs) were colonized by *P. australis*, a species that has a narrow limit with respect to hydroperiod and salinity: seeds germinate in water shallower than 10 cm and with a salinity <5 PSU. *S. alterniflora*, abundant near the shoreline, germinate in water up to 45 cm deep, with salinity tolerance up to 33 PSU. The hydroperiod and salinity conditions are conducive for the establishment of vegetation in the Qingba lobe.

The situation is not the same for the Diaokou or Qingshuigou lobes. In particular, for the Qingshuigou lobe, NDVI values decrease after abandonment, indicating the transition from vegetation to bare ground. Unlike the Qingba lobe, conditions were not hospitable to vegetation. Despite incremental sediment filling since abandonment, the channel remains intertidal, inundated semi-diurnally. Measured salinity values range up to 37 PSU, thus exceeding the tolerance of *P. australis*, and even *S. alterniflora*. Only small *S. salsa* colonies are on the mudflat, varying seasonally with establishment in summer.

Vegetation buffers hydrodynamic energy as the living canopy induces drag and lowers flow velocity (Möller et al., 2014; Nepf, 1999; Nepf et al., 1997, Nepf & Vivoni, 2000). In the subsurface, roots bind sediment, enhance effective cohesion, and provide stability to the landform (Camporeale et al., 2013; Simon & Collison, 2002). Vegetation also enhances accumulation through trapping (Möller et al., 2014). The Qingba lobe displays an abundance of vegetation, particularly compared to the Diaokou and Qingshuigou lobes.

Topography and freshwater input influence vegetation, and therefore play an important role in stabilizing the shoreline of the Huanghe lobes. Insights from this study may be used to inform engineering strategies that seek to mitigate coastal land loss using diversions of water and sediment. An actively prograding delta lobe experiences sediment deposition as the channel bed slope decreases over time (Moodie et al., 2019). It is optimal to relocate engineered channels just upstream of where the channel bed has aggraded. Additionally, the germination depth of native plant species could be used as a metric to determine if the channel bed has aggraded sufficiently for plant colonization following a diversion. Maintaining a riverine water connection to the abandoned lobe is critical to providing freshwater, which nourishes vegetation. Combined, these efforts will stabilize deltaic shorelines and lower lobe retreat rates.

3. Conclusions

The Huanghe delta lobes have been abandoned by avulsions and engineered diversions. In either case, access to water and sediment supply are reduced (if not entirely impeded), and the shoreline recedes. However, the rate at which this occurs, as demonstrated for three recently abandoned lobes, is impacted by vegetal colonization of the delta plain, which damps hydrodynamic processes and minimizes sediment erosion. The key to mitigating shoreline retreat for the Huanghe lobes is therefore to promote vegetal development by ensuring sufficient aggradation of the channel bed and the continued supply of freshwater.

The Huanghe delta exemplifies how engineered diversions sever access to freshwater if located without regard to channel bed elevation. In such a circumstance, hypersaline conditions prevent vegetation from colonizing. Alternatively, the natural avulsion channel is filled with sediment, elevating the topography, with a tie channel that distributes freshwater to the lobe, and vegetation flourishes.

This study highlights effective methods for enhancing shoreline stability of abandoned deltaic lobes. Allowing a channel bed to aggrade to an elevation that supports marsh vegetation along with maintaining connection to freshwater enhances vegetal colonization and sediment stability. Such practices will ensure that engineered diversions of delta lobes produce resilient shorelines.

Data Availability Statement

All code and data used for analyses and conclusions can be obtained online at (https://zenodo.org/deposit/4271925).

Acknowledgments
This study was supported by the National Science Foundation (NSF) EAR-1427262 and EAR-1427259, "Coastal SEES Collaborative Research: Morphologic, Socioeconomic, and Engineering Sustainability of Massively Anthropic Coastal Deltas: The Compelling Case of the Huanghe Delta." The authors would like to thank the Hydrological Survey Bureau of the Yellow River Mouth and the Yellow River Institute of Hydraulic Research for facilitating the logistics of this fieldwork. The authors also gratefully acknowledge field support from Chenliang Wu, Eric Barefoot, Michelle Mullane, Katie Lavalle, Liang Chen, Michael Lamb, and Gary Parker, and graphic design support from Aaron Reeves.

References

Blum, M. D., & Roberts, H. H. (2009). Drowning of the Mississippi Delta due to insufficient sediment supply and global sea-level rise. *Nature Geoscience*, *2*, 488–491. https://doi.org/10.1038/ngeo553

Camporeale, C., Perucca, E., Ridolfi, L., & Gurnell, A. M. (2013). Modeling the interactions between river morphodynamics and riparian vegetation. *Reviews of Geophysics*, *51*(3), 379–414. https://doi.org/10.1002/rog.20014

Carlson, B. N., Nittrouer, J. A., Moodie, A. J., Kineke, G. C., Kumpf, L. L., Ma, H., et al. (2020). Infilling abandoned deltaic distributary channels through landward sediment transport. *Journal of Geophysical Research: Earth Surface*, *125*, e2019JF005254. https://doi.org/10.1029/2019JF005254

Coastal Protection and Restoration Authority. (2017). *Louisiana's comprehensive master plan for a sustainable coast committed to our coast*.

Day, G., Dietrich, W. E., Rowland, J. C., & Marshall, A. (2008). The depositional web on the floodplain of the Fly River, Papua New Guinea. *Journal of Geophysical Research*, *113*(F1), F01S02. https://doi.org/10.1029/2006JF000622

Dong, T. Y., Nittrouer, J. A., McElroy, B., Il'icheva, E., Pavlov, M., Ma, H., et al. (2020). Predicting water and sediment Partitioning in a delta channel network under varying discharge conditions. *Water Resources Research*, *56*(11). https://doi.org/10.1029/2020WR027199

Ganti, V., Chu, Z., Lamb, M. P., Nittrouer, J. A., & Parker, G. (2014). Testing morphodynamic controls on the location and frequency of river avulsions on fans versus deltas: Huanghe (Yellow River), China. *Geophysical Research Letters*, *41*(22), 7882–7890. https://doi.org/10.1002/2014GL061918

Gao, W., Nienhuis, J., Nardin, W., Wang, Z. B., Shao, D., Sun, T., & Cui, B. (2020). Wave controls on Deltaic Shoreline-channel morphodynamics: Insights from a coupled model. *Water Resources Research*. https://doi.org/10.1029/2020WR027298

Gaweesh, A., & Meselhe, E. (2016). Evaluation of sediment diversion design attributes and their impact on the capture efficiency. *Journal of Hydraulic Engineering*, *142*(5), 04016002. https://doi.org/10.1061/(ASCE)HY.1943-7900.0001114

Giosan, L., Syvitski, J., Constantinescu, S., & Day, J. (2014). Climate change: Protect the world's deltas. *Nature*, *516*(7529), 31–33. https://doi.org/10.1038/516031a

Gosselink, J., Coleman, J., & Stewart, R. J. (1998). Coastal Louisiana. In J. Mac, P. A. Opler, C. E. Puckett Haecker, & P. D. Doran (Eds.), Status and trends of the nation's biological resources, U.S. Department of the Interior, U.S. Geological Survey, 385–436.

Hajek, E. A., & Edmonds, D. A. (2014). Is river avulsion style controlled by floodplain morphodynamics?. *Geology*, *42*(3), 199–202. https://doi.org/10.1130/G35045.1

Hiatt, M., Snedden, G., Day, J. W., Rohli, R. V., Nyman, J. A., Lane, R., & Sharp, L. A. (2019). Drivers and impacts of water level fluctuations in the Mississippi River delta: Implications for delta restoration. *Estuarine, Coastal and Shelf Science*, *224*, 117–137. https://doi.org/10.1016/J.ECSS.2019.04.020

Hoitink, A. J. F., Nittrouer, J. A., Passalacqua, P., Shaw, J. B., Langendoen, E. J., Huismans, Y., & Maren, D. S. (2020). Resilience of river deltas in the Anthropocene. *Journal of Geophysical Research: Earth Surface*. https://doi.org/10.1029/2019JF005201

Hoitink, A. J. F., Wang, Z. B., Vermeulen, B., Huismans, Y., & Kästner, K. (2017). Tidal controls on river delta morphology. *Nature Geosciences*, *10*(9), 1–9. https://doi.org/10.1038/NGEO3000

Johnson, W. B., Sasser, C. E., & Gosselink, J. G. (1985). Succession of vegetation in an evolving River Delta, Atchafalaya Bay, Louisiana. *The Journal of Ecology*, *73*(3), 973. https://doi.org/10.2307/2260162

Jones, H. L., & Hajek, E. A. (2007). Characterizing avulsion stratigraphy in ancient alluvial deposits. *Sedimentary Geology*, *202*(1–2), 124–137. https://doi.org/10.1016/j.sedgeo.2007.02.003

Kerr, J. T., & Ostrovsky, M. (2003). From space to species: Ecological applications for remote sensing. *Trends in Ecology & Evolution*, *18*, 299–305. https://doi.org/10.1016/S0169-5347(03)00071-5

Kim, W. (2012). Flood-built land. *Nature Geoscience*, *5*(8), 521–522. https://doi.org/10.1038/ngeo1535

Kim, W., Mohrig, D., Twilley, R., Paola, C., & Parker, G. (2009). Is it feasible to build new land in the Mississippi River Delta?. *Eos, Transactions American Geophysical Union*, *90*(42), 373–374. https://doi.org/10.1029/2009EO420001

Li, Z., Wang, H., Nittrouer, J. A., Bi, N., Wu, X., & Carlson, B. (2020). Modeling the filling process of an abandoned fluvial-deltaic distributary channel: An example from the Yellow River delta, China. *Geomorphology*, 107204. https://doi.org/10.1016/j.geomorph.2020.107204

Luhar, M., & Nepf, H. M. (2013). From the blade scale to the reach scale: A characterization of aquatic vegetative drag. *Advances in Water Resources*, *51*, 305–316. https://doi.org/10.1016/j.advwatres.2012.02.002

Mackey, S. D., & Bridge, J. S. (1995). Three-dimensional model of Alluvial stratigraphy: Theory and application. *Journal of Sedimentary Research*, *65*(1), 7–31. 10.1306/D42681D5-2B26-11D7-8648000102C1865D

Mohrig, D., Heller, P. L., Paola, C., & Lyons, W. J. (2000). Interpreting avulsion process from ancient alluvial sequences: Guadalope-Matarranya system (northern Spain) and Wasatch Formation (western Colorado). *GSA Bulletin*, *112*(3), 1787–1803.

Möller, I., Kudella, M., Rupprecht, F., Spencer, T., Paul, M., Wesenbeeck, Van, B. K., et al. (2014). Wave attenuation over coastal salt marshes under storm surge conditions. *Nature Geoscience*, *7*(10), 727–731. https://doi.org/10.1038/NGEO2251

Moodie, A. J., Nittrouer, J. A., Ma, H., Carlson, B. N., Chadwick, A. J., Lamb, M. P., & Parker, G. (2019). Modeling deltaic lobe-building cycles and channel avulsions for the Yellow River Delta, China. *Journal of Geophysical Research: Earth Surface*, *124*(11), 2438–2462. https://doi.org/10.1029/2019JF005220

Nepf, H. M. (1999). Drag, turbulence, and diffusion in flow through emergent vegetation. *Water Resources Research*, *35*(2), 479–489. https://doi.org/10.1029/1998WR900069

Nepf, H. M., Mugnier, C. G., & Zavistoski, R. A. (1997). The effects of vegetation on longitudinal dispersion. *Estuarine, Coastal and Shelf Science*, *44*(6), 675–684. https://doi.org/10.1006/ecss.1996.0169

Nepf, H. M., & Vivoni, E. R. (2000). Flow structure in depth-limited, vegetated flow. *Journal of Geophysical Research*, *105*(C12), 28547–28557. https://doi.org/10.1029/2000jc900145

Nienhuis, J. H., Ashton, A. D., Roos, P. C., Hulscher, S. J. M. H., & Giosan, L. (2013). Wave reworking of abandoned deltas. *Geophysical Research Letters*, *40*(22), 5899–5903. https://doi.org/10.1002/2013GL058231

Nittrouer, J. A., Shaw, J., Lamb, M. P., & Mohrig, D. (2012). Spatial and temporal trends for water-flow velocity and bed-material sediment transport in the lower Mississippi River. *Geological Society of America Bulletin*, *124*(3–4), 400–414. https://doi.org/10.1130/B30497.1

Olliver, E. A., Edmonds, D. A., & Shaw, J. B. (2020). Influence of floods, tides, and vegetation on sediment retention in Wax Lake Delta, Louisiana. *USA Journal of Geophysical Research: Earth Surface*, *125*, e2019JF005316. https://doi.org/10.1029/2019JF005316

Paola, C., Twilley, R. R., Edmonds, D. A., Kim, W., Mohrig, D., Parker, G., et al. (2011). Natural processes in delta restoration: Application to the Mississippi Delta. *Annual Review of Marine Science*, *3*(1), 67–91. https://doi.org/10.1146/annurev-marine-120709-142856

Piliouras, A., Kim, W., & Carlson, B. (2017). Balancing aggradation and progradation on a vegetated delta: The importance of fluctuating discharge in depositional systems. *Journal of Geophysical Research: Earth Surface*, *122*(10), 1882–1900. https://doi.org/10.1002/2017JF004378

Roberts, H. (1997). Dynamic changes of the Holocene Mississippi River delta Cycle. *Journal of Coastal Research*, *13*(3), 605–627. Retrieved from http://journals.fcla.edu/jcr/article/view/80176/77431

Roelvink, D., Huisman, B., Elghandour, A., Ghonim, M., & Reyns, J. (2020). Efficient modeling of complex sandy coastal evolution at monthly to century time scales. *Frontiers in Marine Science*, *7*, 535. https://doi.org/10.3389/fmars.2020.00535

Rowland, J. C., Dietrich, W. E., Day, G., & Parker, G. (2009). Formation and maintenance of single-thread tie channels entering floodplain lakes: Observations from three diverse river systems. *Journal of Geophysical Research*, *114*(F2), F02013. https://doi.org/10.1029/2008JF001073

Rowland, J. C., Lepper, K., Dietrich, W. E., Wilson, C. J., & Sheldon, R. (2005). Tie channel sedimentation rates, oxbow formation age and channel migration rate from optically stimulated luminescence (OSL) analysis of floodplain deposits. *Earth Surface Processes and Landforms*, *30*(9), 1161–1179. https://doi.org/10.1002/esp.1268

Shao, Y., Lunetta, R. S., Wheeler, B., Iiames, J. S., & Campbell, J. B. (2016). An evaluation of time-series smoothing algorithms for land-cover classifications using MODIS-NDVI multi-temporal data. *Remote Sensing of Environment*, *174*, 258–265. https://doi.org/10.1016/j.rse.2015.12.023

Shaw, J. B., & Mohrig, D. (2014). The importance of erosion in distributary channel network growth, Wax Lake Delta, Louisiana, USA. *Geology*, *42*(1), 31–34. https://doi.org/10.1130/G34751.1

Simon, A., & Collison, A. J. C. (2002). Quantifying the mechanical and hydrologic effects of riparian vegetation on stream bank stability. *Earth Surface Processes and Landforms*, *27*(5), 527–546. https://doi.org/10.1002/esp.325

Slingerland, R., & Smith, N. D. (2004). River avulsions and their deposits. *Annual Review of Earth and Planetary Sciences*, *32*, 257–285. https://doi.org/10.1146/annurev.earth.32.101802.120201

Sun, C., Fagherazzi, S., & Liu, Y. (2018). Classification mapping of salt marsh vegetation by flexible monthly NDVI time-series using Landsat imagery. *Estuarine, Coastal and Shelf Science*, *213*, 61–80. https://doi.org/10.1016/J.ECSS.2018.08.007

Syvitski, J. P. M., Kettner, A. J., Overeem, I., Hutton, E. W. H., Hannon, M. T., Brakenridge, G. R., et al. (2009). Sinking deltas due to human activities. *Nature Geoscience*, *2*(10), 681–686. https://doi.org/10.1038/ngeo629

Taha, Z. P., & Anderson, J. B. (2007). The influence of valley aggradation and listric normal faulting on styles of river avulsion: A case study of the Brazos River, *Geomorphology*, *95*(3), 429–448. https://doi.org/10.1016/j.geomorph.2007.07.014

Törnqvist, T. E., Wallace, D. J., Storms, J. E. A., Wallinga, J., Dam, Van, R. L., Blaauw, M., et al. (2008). Mississippi Delta subsidence primarily caused by compaction of Holocene strata. *Nature Geoscience*, *1*(3), 173–176. https://doi.org/10.1038/ngeo129

Wagner, W., Lague, D., Mohrig, D., Passalacqua, P., Shaw, J., & Moffett, K. (2017). Elevation change and stability on a prograding delta. *Geophysical Research Letters*, *44*(4), 1786–1794. https://doi.org/10.1002/2016GL072070

Wilson, C. A., & Allison, M. A. (2008). An equilibrium profile model for retreating marsh shorelines in southeast Louisiana. *Estuarine, Coastal and Shelf Science*, *80*, 483–494. https://doi.org/10.1016/j.ecss.2008.09.004

Wu, X., Wang, H., Bi, N., Nittrouer, J. A., Xu, J., Cong, S., et al. (2020). Evolution of a tide-dominated abandoned channel: A case of the abandoned Qingshuigou course, Yellow River. *Marine Geology*, *422*. https://doi.org/10.1016/j.margeo.2020.106116

Xing, F., Syvitski, J. P. M., Kettner, A. J., Meselhe, E. A., Atkinson, J. H., & Khadka, A. K. (2017). Morphological responses of the Wax Lake Delta, Louisiana, to Hurricanes Rita. *Elementa: Science of the Anthropocene*, *5*(0), 80. https://doi.org/10.1525/elementa.125

Xu, H. (2006). Modification of normalised difference water index (NDWI) to enhance open water features in remotely sensed imagery. *International Journal of Remote Sensing*, *27*(14), 3025–3033. https://doi.org/10.1080/01431160600589179

Yu, L. (2002). The Huanghe (Yellow) River: A review of its development, characteristics, and future management issues. *Continental Shelf Research*, *22*(3), 389–403. https://doi.org/10.1016/S0278-4343(01)00088-7

Zhang, J. Z., Huang, H., & Bi, H. (2014). Land subsidence in the modern Yellow River Delta based on InSAR time series analysis. *Natural Hazards*, *75*(3), 2385–2397. https://doi.org/10.1007/s11069-014-1434-7

References From the Supporting Information

Ashton, A. D., & Murray, A. B. (2006). High-angle wave instability and emergent shoreline shapes: 1. Modeling of sand waves, flying spits, and capes. *Journal of Geophysical Research*, *111*(F4), F04011. https://doi.org/10.1029/2005JF000422

Didan, K. (2015). MOD13Q1 MODIS/Terra vegetation Indices 16 day L3 Global 250 m SIN Grid V006. https://doi.org/10.5067/MODIS/MOD13Q1.006

Mullane, M., Kineke, G. C., Kumpf, L. L., & Carlson, B. N. (2020). Seasonal wave attenuation in the muddy nearshore environment of the modern Huanghe Delta from in situ observations and SWAN modeling. *Ocean Sciences Meeting*.

Zhang, P., Li, Z., & Wen, H. (2012). Modernization of National Geodetic Datum in China. Nineteenth United Nations Regional Cartographic Conference for Asia and the Pacific. *United Nations Economic and Social Council*, 1–6.